Electron-Diffraction Structural Study of Polymeric Gaseous Hydrogen Fluoride*

JAY JANZEN† AND L. S. BARTELL

Department of Chemistry, University of Michigan, Ann Arbor, Michigan 48104

(Received 15 November 1968)

Electron diffraction patterns with molecular interference features extending beyond $s=35$ Å^{-1} were obtained for gaseous self-associated HF introduced under its own vapor pressure at $-19°$ and at $+22°$C through a conventional nozzle system into a 40-kV electron beam. The diffraction patterns and their dependence on temperature are best explained with the hypothesis that the monomer and a puckered, cyclic hexamer were the only appreciable constituents of the scattering vapors. Mean FFF angles in the hexamer were found to be only about 104°, in contrast with the 120° angles reported for the infinite planar zigzag chains in crystalline HF at $-125°$C. This pucker may simply be a consequence of thermal bending of the extremely flexible ring. Indeed, the experimental radial distribution function is so smeared out by large ring-bending amplitudes that the data cannot distinguish between boatlike and chair conformations. It is likely that the free $(HF)_6$ molecules sweep randomly through both conformations in their thermal undulations. At the two temperatures studied the hydrogen-bonded FF distances were 2.525 and 2.533 Å, with standard errors of 0.003 Å, in comparison with the solid-state result of 2.49 ± 0.01 Å. Corresponding FF amplitudes of vibration were 0.089 and 0.101 Å (±0.003 Å), respectively. Perhaps 70% at $-19°$ and 45% at 22° of the hydrogen bonds were asymmetric with covalent FH distances 0.04_0 Å longer than those in the monomer molecules. The data suggest, however, that the remainder of the ring protons migrate a substantial distance off-axis to a more symmetrical disposition between the fluorines.

INTRODUCTION

The enormous importance of hydrogen bonds in chemical and biological systems has stimulated intensive study of their properties. Only a minute fraction of the structural studies to date have involved free complexes in the vapor phase; they have been devoted, instead, to the solid state, where considerations of molecular packing may complicate interpretations. An examination of gaseous systems would therefore seem to be of special interest. One of the most promising of these systems is hydrogen fluoride, for which the manifestations of hydrogen bonding are striking and for which, by virtue of its essential simplicity, there is the greatest hope of bridging the gap between experiment and *ab initio* theory. Because investigations by various methods, including an early visual electron diffraction study, had not yet led to agreement on the nature of the gas phase polymeric species, a re-examination of the vapors of hydrogen fluoride by electron diffraction seemed warranted. Modern techniques of electron diffraction lend themselves well to the study of geometries of gaseous molecules in the pressure range of appreciable HF polymer formation.

This paper describes the experimental conditions, analysis of data, and results of HF studies conducted at nominal temperatures of $-19°$ and $+22°$C. The diffraction data by themselves lead to a suggestive but not unique set of conclusions. When they are augmented by inferences from other sources of data,[1,2] however, a particularly simple and strongly supported interpretation is reached. A critical review of the prior research on HF vapor has appeared elsewhere.[1]

EXPERIMENTAL PROCEDURE

Electron-diffraction experiments for this study were conducted to obtain structural data for gaseous hydrogen fluoride in as highly polymerized a form as was feasible. Accordingly, diffraction patterns were recorded using relatively large sample pressures to favor a high degree of association in the vapor jet of the specimen. Data were collected at two temperatures to furnish clues to whatever changes might occur with changing association factor.

In the problem at hand, the conventional index of resolution R which measures experimental efficiency is not separable from structural (distance multiplicity) and concentration unknowns which have to be determined from the experimental data. Therefore R was initially fixed at the ideal value 1.0 as a working assumption. Attention was then given in the analysis to possible pressure-related and other effects capable

* This research was supported by a grant from the National Science Foundation. For a complete tabulation of experimental intensity data, order document NAPS-00256 from ASIS National Auxiliary Publications Service, c/o CCM Information Sciences, Inc., 22 West 34th Street, New York, N.Y. 10001, remitting $1.00 for microfiche or $3.00 for photocopies.

† Present address: Chemical Laboratory, Phillips Petroleum Company Research Center, Bartlesville, Okla. 74003.

[1] J. Janzen and L. S. Bartell, U.S. Atomic Energy Commission, IS-1940, 47 pp., 1968. This supplement of the present study reviews relevant HF literature, refines and extends published analyses, and concludes in favor of the description of Ref. 2, below. The essential conclusions are that the principal constituents of HF vapor are monomer, dimer, and a cyclic hexamer, and that the amount of dimer is minor under the present conditions. The existence of other oligomers is likely, but in concentrations which are, for most nonspectroscopic experimental purposes, completely negligible by comparison with the $HF+(HF)_2+(HF)_6$ total at room temperature and below. The possibility of ring formation from six-membered chains at a very small cost in entropy of ring closure is viewed as the source of special stability which makes the cyclic hexamer the predominating polymeric species.

[2] E. U. Franck and F. Meyer, Z. Elektrochem. **63**, 571 (1959).

TABLE I. Experimental conditions for HF diffraction photographs.

Approx. temp. (°C)	+22			−19		
Approx. vapor pressure[a] (torr)	830			163		
Electron wavelength (Å)	0.06015			0.06015		
Nozzle orifice diam (mm)	0.20			0.28		
Beam current (μA)	0.364			0.385		
Plates taken at	Iowa State University			University of Michigan		
Date	1965			1966		
Sector	Quadratic	Cubic	Cubic	Quadratic	Cubic	Cubic
Nozzle-to-plate distance (mm)	210.50	210.54	108.81	209.15	209.23	106.99
Exposure time (sec)	0.1	0.8–1.0	2	0.5	5	12
Number of plates averaged	7	5	5	4	4	4

[a] R. L. Jarry and W. Davis, Jr., J. Phys. Chem. **57**, 600 (1953), Eq. (1).

of reducing R and influencing the structural conclusions derived.

Apparatus and Materials

Two series of electron-diffraction photographs[3] of HF vapor were made using an apparatus described elsewhere.[4,5] The sample was introduced from a valved reservoir containing liquid HF directly connected to the inlet line; the effective sample pressure upstream from the nozzle was therefore as near to the saturation vapor pressure as could conveniently be arranged. During the first series of experiments the sample container and injection line were at the ambient laboratory temperature, approximately 22°C. For the second series, the inlet tubing and sample reservoir were enclosed in a jacket through which a coolant (dried air chilled in a dry-ice slush) could be circulated. With this arrangement the sample cell and the upstream end of the injection line were held at approximately −19°C, while the nozzle end of the line was at about −37°C. The temperature gradient was mostly due to thermal contact between the cooling jacket and the vacuum wall of the diffraction chamber and could not be easily avoided. The effect of a temperature decrease in the direction of sample flow was presumably advantageous in these experiments, however, because it would tend to counter the dissociative effect of the inevitable pressure drop in the same direction.

Anhydrous liquid hydrogen fluoride was supplied in lecture bottles by the Matheson Company, Inc. Purity of the liquid phase was specified by the manufacturer to be at least 99.9 mole %. The material was used without further purification, except whatever may have incidentally attended filling of the sample cells by vacuum distillation at 0°C.

The sample system[6] used for the room-temperature experiments was made entirely of Kel-F, excepting the nozzle tip, which was platinum. The jacketed low-temperature injection system had Teflon gaskets at all joints and a nozzle tip of nickel, but was otherwise of Monel metal. The transfer line through which the sample cells were filled consisted of nickel tubing silver-soldered to Monel metal Hoke bellows valves which were fitted with Teflon gaskets.

Recording Diffraction Patterns

Data in the interval $3.2<s<40.5$ Å^{-1} were obtained from photographs made at nozzle-to-plate distances nominally 21 and 11 cm with the usual radius-cubed rotating sector.[4,7] Corrections for imperfections in the shape of this sector were made according to the argon-based calibration previously in routine use in this laboratory. Additional data for $2.1<s<14.9$ were taken at the 21-cm distance using a radius-squared (quadratic) sector of 34-mm maximum radius. This sector was calibrated with neon, which is isoelectronic with HF, and the calibration curve agreed well with the results of an optical calibration done earlier.[8] Background functions for the leveled quadratic-sector data were quite smooth, though not horizontal, throughout the s range from ~2.1 to ~15; they displayed the tendency to bend near $s=7$ that has been noted previously.[7,9]

Diffraction patterns were recorded on 4×5-in. Kodak Process Plates. An approximate correction[10] to remove the "edge effect" which these plates exhibit[11,12] was

[3] The Ph.D. thesis of J. Janzen (Iowa State University, 1968) may be consulted for additional details.

[4] L. S. Bartell, Kozo Kuchitsu, and R. J. deNeui, J. Chem. Phys. **35**, 1211 (1961).

[5] B. L. Carroll, unpublished Ph.D. thesis, Iowa State University, Ames, Iowa, 1963, pp. 5–8.

[6] J. P. Guillory, unpublished Ph.D. thesis, Iowa State University, Ames, Iowa, 1965, p. 60.

[7] S. Shibata and L. S. Bartell, J. Chem. Phys. **42**, 1147 (1965).

[8] L. S. Bartell and L. O. Brockway, Phys. Rev. **90**, 833 (1953).

[9] L. S. Bartell, D. A. Kohl, B. L. Carroll, and R. M. Gavin, Jr., J. Chem. Phys. **42**, 3079 (1965).

[10] D. J. Dahm (personal communication, Ames, Iowa, 1965).

[11] D. A. Kohl and R. A. Bonham, J. Chem. Phys. **47**, 1634 (1967); D. A. Kohl, unpublished Ph.D. thesis, Indiana University, Bloomington, Ind., 1966), Chap. V.

[12] L. S. Bartell and L. O. Brockway, J. Appl. Phys. **24**, 656 (1953).

applied through division of observed optical densities measured at distances y more than 24 mm from the center of a plate by $[1+0.000125(y-24)^2]$. All densities were then converted to values of exposure E according to the emulsion calibration equation[3]

$$E=D+0.05D^3.$$

Additional information concerning experimental conditions appears in Table I.

Extraneous Intensities

During at least one typical experimental run with each configuration of the apparatus, a blank exposure was made in the absence of specimen flow to record extraneous internsities. Residual gas pressure during a blank exposure was always between 10^{-5} and 4×10^{-5} torr. The extraneous intensity corrections indicated by such blanks were trivial, typically only about 0.2% of the total HF diffraction pattern intensities.

Even through sample pressures greater than 1 atm were used, the background pressure in the diffraction chamber remained below 10^{-3} torr during sample injection, as indicated by a hot-cathode ionization gauge. Greatly augmenting the specimen removal was a large (>1000 cm²) liquid-nitrogen-cooled surface beyond the nozzle exit. It may be supposed that the blanks described above underestimate the true extraneous intensities effective during an actual diffraction exposure, because the contribution of scattering by delocalized specimen gas was absent. An experimental attempt to assess the scattering to be expected

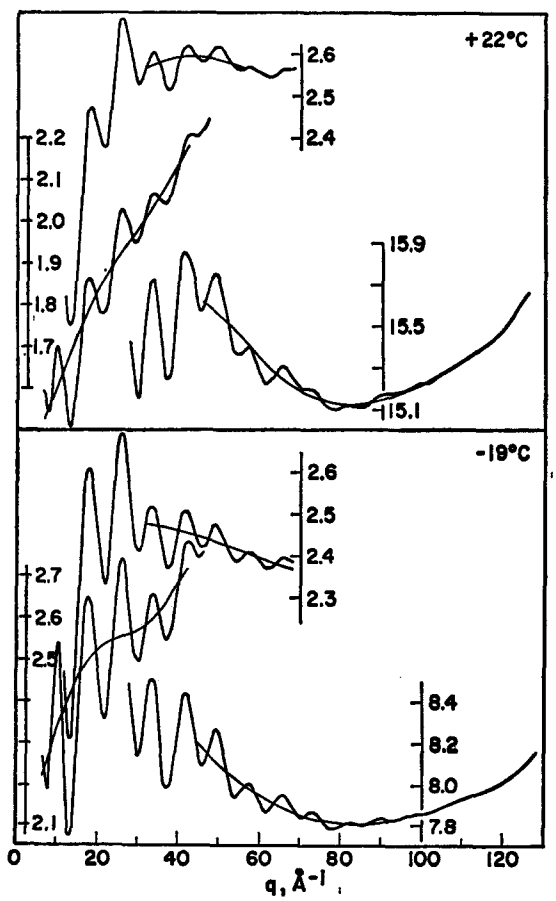

FIG. 1. Leveled experimental total intensities and background functions for hydrogen fluoride vapor at nominal temperatures of +22° and −19°C. Data shown were leveled and corrected for sector asperities as described in Ref. 16.

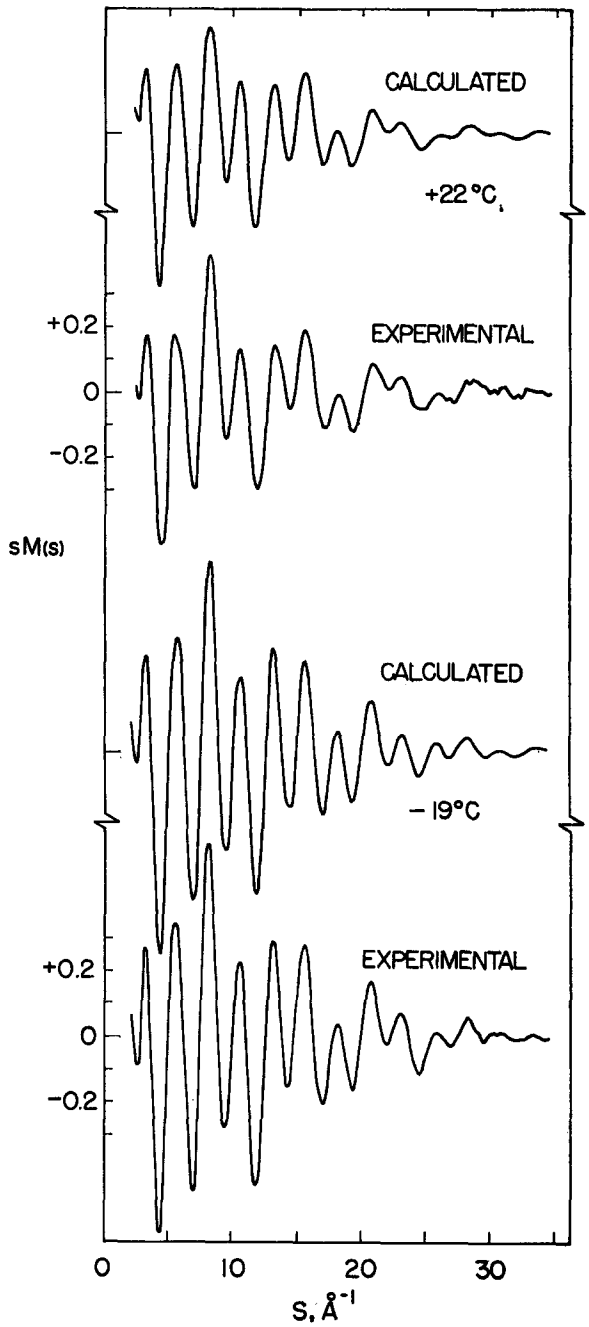

FIG. 2. Reduced molecular intensity curves $sM(s)$ for hydrogen fluoride vapor. Calculated curves are based on a model with some of the protons delocalized to off-axis regions equidistant between the fluorines (see text).

in the present work from delocalized HF was made by a method similar to one outlined elsewhere.[13] A plate was exposed under the same conditions used for the long-distance, quadratic-sectored HF plates taken at −19°C, except that the electron beam was aligned to pass about 2 mm to the side of and slightly behind the exit end of the nozzle. The pattern on this plate was faint and similar in shape to the analogous exposure patterns taken with the electron beam directly intersecting the stream from the nozzle, but it was less than 3% as strong (i.e., five to eight times the ordinary blank intensity). From these observations it seems reasonable to conclude that neglect of corrections for delocalized extraneous scattering in this study would result[14] in a diminution of not more than 3%–4% in the indices of resolution. Data obtained in the delocalized-scattering experiment also indicate that extraneous scattering may contribute appreciably to the upsweep of backgrounds at larger scattering angles.[15]

Reproducibility

Despite the unfavorable experimental conditions imposed to obtain high concentrations of polymer, reproducibility of the molecular scattering patterns from plate to plate and from one apparatus configuration to another was virtually as good as that heretofore achieved in this laboratory.[3]

Over-all confidence in the results from the two sets of photographs is enhanced by noting their extensive similarities, to be discussed below, which persisted through not only a lowering of the temperature, but also the dismantling and relocation of the diffraction unit, use of samples from different manufacturer's batches, a change in container materials, alterations in the microphotometer detector circuitry, and lapse of a year's time between the sets of experiments.

Preliminary Reduction of Data

Leveled experimental intensities, reduced molecular intensities $M(s)$, and radial distribution functions $f(r)$ were obtained from the photographic exposure data by methods similar to those described elsewhere.[16,17] The Degard damping factor used for computing experimental $f(r)$ curves was $\exp(-0.00125s^2)$.

RESULTS AND DISCUSSION

Results of the diffraction experiments are depicted in Figs. 1–3. The final experimental radial distribution functions appear in Fig. 3 as solid curves. Each $f(r)$ curve consists of four peaks, none unambiguously resolvable into components, which will be referred to hereafter by number from left to right. The diffraction data consisting of more than 6000 intensity measurements can be satisfactorily explained with the assumption of a single species to represent the oligomers in the scattering vapor. That species has a skeleton of fluorine atoms in the form of a flexible six-membered ring. After least-squares refinement of the parameters defining such a model, the rms deviation between observed and calculated intensities was of the order of two parts per thousand. Differences between theoretical and experimental $f(r)$ curves are plotted at the bottom of Fig. 3 and do not exceed common levels of $f(r)$ noise.

Inferences from Peak Areas

Before discussing further the characteristics of the favored model it will be useful to outline some of the reasoning, including unfavorable aspects of possible alternative interpretations, which led to its adoption. It should be borne in mind throughout the discussion that this type of analysis of a mixed vapor, for which neither composition nor possible structures of the components is known in advance, is more difficult and subject to greater uncertainty than conventional electron diffraction analyses.

At the outset it was assumed that association factors found by vapor density measurements on saturated vapor could be used as rough estimates of upper bounds on molecular weight averages likely to be encountered in the diffraction experiments. Within the limits of this assumption, but without geometric or

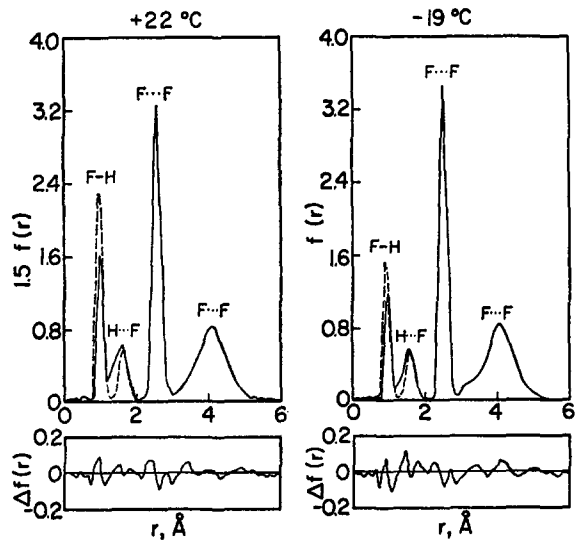

FIG. 3. Radial distribution functions. Solid curves are from Fourier inversion of experimental data. Dashed curves represent calculated functions based on the assumption that each hydrogen bond is asymmetric with a proton more or less localized on the F···F axis. A significantly better fit was obtained if some of the protons were delocalized to off-axis regions roughly equidistant between fluorines.

[13] Reference 4, footnote 7.
[14] L. S. Bartell, J. Appl. Phys. **31**, 252 (1960).
[15] Compare Fig. 1 of the present paper with that of L. S. Bartell and J. P. Guillory, J. Chem. Phys. **43**, 647 (1965). Recall that a correction for the edge effect was applied in the present study.
[16] R. A. Bonham and L. S. Bartell, J. Chem. Phys. **31**, 702 (1959).
[17] R. A. Bonham and T. Ukaji, J. Chem. Phys. **36**, 72 (1962).

mass conservation constraints, a mathematical model was used in the process of $f(r)$ refinement until good, physically interpretable $f(r)$ results were obtained. The refinement proceeded at first by pure trial and error, and then by a cyclic process of adjusting the model, peak areas and all, to agree with the experimental $f(r)$ followed by improvement of background functions under smoothness and nonnegative $f(r)$ criteria. This process of refining $f(r)$ continued until the approximate geometrical characteristics of the oligomer fluorine skeleton become clear; only then were peak areas and geometric consistency corresponding to a particular physical model introduced and the model refined by least-squares fitting of the observed intensities and by continued visual comparison of experimental and calculated $f(r)$ curves. Because solution of the structure depends heavily on the experimental $f(r)$ peak areas, it is gratifying that the development of the experimental $f(r)$ curves converged to give physically-interpretable results in the absence of area constraints such as are tactily adopted in routine work. Indeed, the areas of experimental peaks 1–4 appeared sufficiently insensitive to the assumed model so that their uncertainties could be roughly estimated as $<8\%$, $<10\%$, 5%, and 30%, respectively. As expected, the broadest peaks have the most uncertain areas.

The observed areas of peaks 3 and 4 at once suggest in a straightforward way the qualitative conclusions to be drawn concerning gross geometry of the oligomer fluorine atom skeleton. In the low-temperature instance, the area of experimental peak 3, which represents the hydrogen-bonded FF distances, is too large, relative to the maximum number $j-1$ of such distances possible in an acyclic species of length j monomer units, for the data to be explained in terms of any mixture having a plausible association factor and containing only acyclic (chain-type) species. The data might be fitted with a chain-only model if the association factor were taken near 7, but that is well above the largest reasonable value (i.e., $\lesssim 5$ even in saturated vapor at -50°C).[1] On the other hand, the -19°C data are well represented by an equimolar mixture of monomer with cyclic hexamer. The association factor of this $1HF+1(HF)_6$ model is 3.5, a value not exceeding the saturation limit at any temperature below $+5$°C; at -19°C the limiting value is ≈ 4.1.

The third $f(r)$ peak in the room-temperature curve is not large enough to show insufficiency of acyclic models by means of the same argument, but the similarities between the radial distribution functions for the two temperatures justify the assumption that the same sort of model should be applicable in both cases. Furthermore, the very similarity of the two polymer patterns (peaks 2–4) is itself an important clue. The 22° curve of Fig. 3 is plotted on a vertical scale expanded 1.5 times so that the shapes of the two observed radial distribution functions can be readily compared. The *shape* of the polymer pattern changes

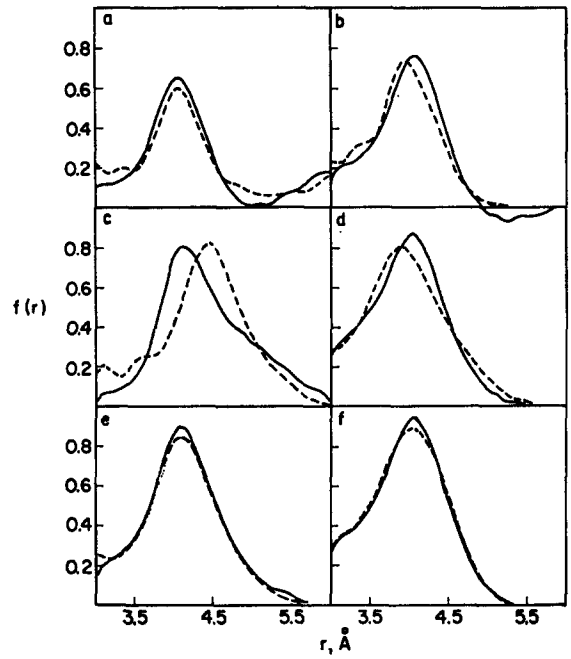

FIG. 4. Non-hydrogen-bonded F···F distribution peak for -19°C sample. The solid lines represent the experimental curve; the dashed lines are calculated for various model structures. (a) Planar zig-zag chains. (b) Planar cyclic pentamer (puckering would worsen fit). (c) Planar cyclic hexamer. (d) Cyclic hexamer, chair conformation, $\angle FFF = 100°$. (e) Cyclic hexamer, boat conformation, $\angle FFF = 106°$. (f) Cyclic hexamer, chair conformation, $\angle FFF = 102.5°$. Experimental curves shift slightly with model owing to use of calculated intensities in inaccessible small-angle region.

very little on lowering the temperature by at least 41°, while the *intensity* of polymer features increases appreciably, as is also apparent in Fig. 2. This is the behavior to be expected of a single associated species mixed with monomer in temperature-dependent proportions. If the polymers were principally open chains whose average length increased with increasing association factor, the temperature difference of the diffraction experiments might be expected to produce significant dissimilarities between the distributions of long nonbonded (peak 4) distances. That peak 4 does not appreciably shift position with temperature is apparent from the data. There is also no indication that the ratio of areas of peaks 3 and 4 is temperature dependent, although a possibility of a modest dependence remains because of uncertainties in the areas of the extremely broad fourth peaks. Nevertheless, an extended planar zigzag chain model with an association factor less than 5 cannot account for more than 40% of the peak 4 area displayed for -19°C in Fig. 3, or 83% of the dashed-curve area (which is already too small) of Fig. 4(a). This weighs heavily against such a model, and the discrepancy in Fig. 4(a) can only become worse if the association factor is lowered from 6.0 to a more reasonable value.

The foregoing considerations show only that the diffracted-intensity data seem incompatible with models

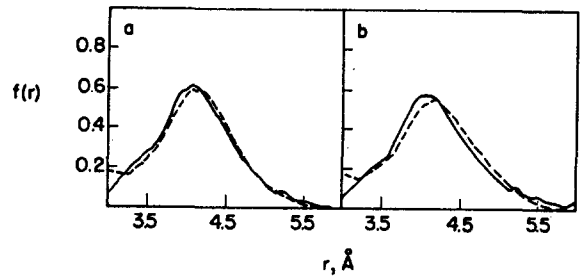

FIG. 5. Non-hydrogen-bonded F···F distribution peak for +22°C sample. Solid lines, experimental; dashed lines, calculated for cyclic hexamer, ∠FFF = 109.5°. (a) Boat conformation. (b) Chair conformation. A better fit is obtained for slightly smaller angles.

containing no cyclic species. Because of experimental uncertainties, there remains the possibility that appreciable concentrations of chain-type species could exist together with cyclic ones and not be discernible in the diffraction experiments. An important point to be noted here is that the arguments and conclusions of the preceding two paragraphs are strengthened rather than weakened if the true index of resolution R should turn out to be less than unity owing to non-optimum conditions (such as multiple scattering in the comparatively dense sample jet).

The curious deficiencies of area under peak 1 to be discussed later[18] raise the question of whether or not indices of resolution below unity are indicated. Peak 3 of the low-temperature $f(r)$ curve furnishes an independent, more reliable, internal estimate of the maximum possible cumulative lowering effect on R by all influences. An R value of less than 0.84 could account for peak 1. Such a low value does not seem reasonable, given that the area of the third low-temperature peak is only ~5% uncertain and that the association factor does not exceed 5. It seems inconceivable that contaminants could have been introduced into the experiment in sufficient quantity to affect this conclusion. Nevertheless, even if appreciable contamination could have occurred, the most plausible impurities (air, water, and SiF_4) are incapable of accounting for the 20%–30% amounts by which peak 1 appears to be deficient.

Theoretical fourth $f(r)$ peaks for a few typical nearly adequate trial models which were investigated are compared with experimental results in Figs. 4 and 5 where the inadequacies of these alternative models are evident. Characteristics of the model favored on the basis of the data are discussed below and are summarized in Table II.

Composition

The readily apparent enhancement of the molecular scattering features (Fig. 2) and $f(r)$ peak areas (Fig. 3) which results from lowering the sample temperature is necessarily interpreted in terms of an increase in the degree of association, rather than a change in R associated with the reduction in sample pressure from the large value used at 22°C; this conclusion follows from quantitative consideration of the $f(r)$ peak areas. For each experimental temperature, Table II gives the proportions of monomer and cyclic hexamer deduced in a least-squares fitting of the data. The corresponding association factors are both plausible values. Moreover, both are large enough to justify the neglect of aggregates other than the cyclic hexamer in analyzing the data, because the expected dimer contributions[19] are at or below the level of noise in $f(r)$ and uncertainties in indices of resolution.

Hydrogen-Bonded Fluorine–Fluorine Distances

The dominant features of the diffraction pattern correspond to the 2.5-Å hydrogen-bonded FF distance, to be referred to hereafter as F_1F_2. This distance

TABLE II. Structural parameters from least-squares fitting of intensities.

Temp. of sample cell	−19°C	+22°C
Sample composition	1.0 HF+$(HF)_6$	4.2 HF+$(HF)_6$
Association factor	3.50	1.96
$r_g[F-H\ 1b]$[a]	0.973±0.009 Å	0.973±0.009 Å
$\Delta r[F-H]$[b]	0.04±0.009 Å	0.04±0.009 Å
$r_g[F_1F_2]$[c]	2.525±0.003 Å	2.535±0.003 Å[d]
$l_m[F_1F_2]$[c]	0.089±0.003 Å	0.101±0.003 Å
$r_g[F_1\cdots F_3]$[e]	3.94±0.05 Å	3.88±0.06 Å
$l_m[F_1\cdots F_3]$	0.39±0.06 A	0.36±0.06 Å
$r_g[F_1\cdots F_4]$[e]	4.37±0.14 Å	4.40±0.11 Å
$l_m[F_1\cdots F_4]$	0.33±0.08 Å	0.30±0.10 Å
"Anomalous" protons[f]	23%	34%
Dimer contribution[g]	0.6%	3.5%

[a] Shortest FH distance in the polymer.
[b] Increase in above distance over monomer r_g bond length.
[c] The r_g and l_m notation is as in Ref. 25.
[d] A better $f(r)$ fit is obtained if this distance is taken as 2.531 Å.
[e] Based on assumption of chair-type conformation.
[f] Deficiency in peak 1 and surplus in peak 2, percent of total hydrogens in sample.
[g] Contribution to polymer $M(s)$, estimated from data in the literature; cf. Ref. 2.

[18] Refer to subsequent section on "···distances less than 2 Å."

[19] An examination of the literature (Ref. 1) disclosed no compelling evidence for the existence, in vapors at equilibrium, of any other polymeric species which could make larger contributions. See specifically Appendix A of Ref. 1 and Fig. 12 of Ref. 2. Note, also, that in the final adiabatic free expansion of the gas jet into the vacuum chamber, it is expected that the temperature will drop markedly as the pressure drops. This expansion lasts only for about a microsecond before the electron beam is encountered. Even if it is assumed that equilibrium is maintained, no gross change in monomer–hexamer ratio is expected. From the heat capacities and heats of polymerization summarized in Refs. 1 and 2, it can be calculated that the effects of T and P changes nearly cancel each other insofar as equilibrium composition is concerned.

(2.533 Å at 22°C, 2.525 at −19°C) is well defined by the data and is consistent with the 2.49±0.01-Å distance found in crystalline HF at −125°C by x-ray diffraction.[20] The mean distance and its vibrational amplitude may increase slightly with temperature.

Non-Hydrogen-Bonded Distances and Configuration

The fourth $f(r)$ peaks consist mostly of unresolved F_1F_3 and F_1F_4 components smeared out by large amplitudes of vibration. Near-zero restoring forces for $F_1F_2F_3$ angles are consistent with theoretical predictions.[21]

The average F_1F_3 distance corresponds to an $F_1F_2F_3$ angle of ≈104° (or ≈102.5° for pure chair conformations, ≈105.5° for pure boat). Such an angle is significantly smaller than the 120.1° angles found in the crystal structure,[20] and in marked disagreement with the value 140±5° reported in the earlier electron-diffraction study.[22] In view of the large vibrations involved, sizable F_1F_3 shrinkage effects[23] may be expected, and it is entirely possible that, in its *equilibrium* configuration, the ring of fluorine atoms is planar, with FFF angles the same as those found in crystalline chains. The amount of shrinkage necessary to reduce the apparent angle from 120° to 104° is of the order of only 9%. Skrinkages exceeding 3% have already been observed for comparably large distances in the presumably much more rigid C_2O_3 structure.[24] Although the hexameric ring is plainly puckered rather than "benzenelike" in the mean distances it displays, insufficient information is available to distinguish boat from chair, or other, conformations. It is probable, however, that a broad continuum of conformations is swept through as the exceedingly flexible ring vibrates.

Nonbonded FH distances greater than 2 Å and all HH distances give minor contributions buried in the $f(r)$ peaks and cannot be deduced directly from the diffraction data. In the data analysis, approximate values for these distances were reckoned from the geometry of the fluorine skeleton and were then formally included in computations to give consistent $f(r)$ peak areas. The distance values used have no experimental significance, and errors therein do not appreciably affect the experimental outcome.

Distribution of Fluorine–Proton Distances Less than 2 Å

Structure parameters for the monomer were taken from the literature[25,26] and were not varied in the analysis. The monomer FH internuclear distance contributes to $f(r)$ peak 1; subtraction of the monomer contribution leaves a component (to be called peak 1b) representing a slightly elongated FH distance (see Δr in Table II). The mean amplitude for the residual polymer component 1b does not differ from that of the monomer (l_m=0.066 Å) by more than the experimental error.

Relative to the expected[27] equal-multiplicity contributions to peaks 1b and 2 by every proton in the oligomer structure, experimental peak 1 is deficient in area by 23% at −19° (a deficiency of 27% of the ring protons) and by 34% at 22° (55% of the ring protons), while a compensating amount of excess area appears in each case under peak 2. Direct least-squares fits of the diffracted intensities (in which both the background function[9] and the relative proton concentrations were varied) yielded a similar result. If this area shift is genuine, the implication is that the average oligomer structure contains a sizable, temperature-dependent fraction of protons located in the region of space between two fluorines at a distance well beyond 1 Å from the nearest fluorine neighbor. According to this interpretation, peak 2 would consist of three components. Unfortunately, an unambiguous resolution is not possible. Qualitatively, however, the center of gravity of the excess contribution to peak 2 appears to be at more than half the F_1F_2 distance. This would imply large protonic excursions away from F_1F_2 internuclear axes, and the observed anomalous peak area behavior is consistent with the existence of a low-lying secondary minimum in the potential-energy field in which a H-bonding proton moves. In this connection it may be mentioned that spectroscopic properties of hydrogen bonds are not yet well understood and that large, unexplained temperature effects on infrared spectra have been reported previously.[28] A relationship between the "tetramer bands" reported by Smith[29] and the "proton shift" under consideration here could conceivably exist, but has not been investigated. Not all aspects of the infrared and Raman HF crystal spectra have been accounted for,[30] nor were the hydrogens located precisely in the x-ray study.[20]

The results concerning shifts of area from peak 1 to 2 are accepted with reservation because it is not impossible that experimental or interpretational complications are responsible. Attempts to devise plausible alternative explanations, however, have failed, leaving at least a strong possibility that, on the average, some of the FH-bonded distances are severely elongated. In any event, the present study suggests the possible

[20] M. Atoji and W. N. Lipscomb, Acta Cryst. **7**, 173 (1954).
[21] B. B. Howard, J. Chem. Phys. **39**, 2524 (1963), Fig. 2.
[22] S. H. Bauer, J. Y. Beach, and J. H. Simons, J. Am. Chem. Soc. **61**, 19 (1939).
[23] Y. Morino, S. J. Cyvin, K. Kuchitsu, and T. Iijima, J. Chem. Phys. **36**, 1109 (1962).
[24] Y. Morino, K. Kuchitsu, and M. Tanimoto (to be published).
[25] K. Kuchitsu and L. S. Bartell, J. Chem. Phys. **35**, 1945 (1961).
[26] G. Herzberg, *Spectra of Diatomic Molecules* (D. Van Nostrand Co., Inc., Princeton, N.J., 1950), 2nd ed., p. 536.
[27] See dashed curves of Fig. 3.
[28] R. H. Hughes, R. J. Martin, and N. D. Coggeshall, J. Chem. Phys. **24**, 489 (1956), and D. Hadzi, Ed., *Hydrogen Bonding* (Pergamon Press, Inc., New York, 1959).
[29] D. F. Smith, J. Phys. Chem. **28**, 1040 (1958).
[30] J. S. Kittelberger and D. F. Hornig, J. Chem. Phys. **46**, 3099 (1967).

fruitfulness of further research on the spatial distribution of hydrogen-bonding protons.

CONCLUSION

Electron diffraction does not by itself lead unequivocally to a unique solution for composition and molecular structure in self-associated hydrogen fluoride vapor, but the data are compatible with a model in which a cyclic hexamer exists as the predominant aggregate species. A similar statement also applies to a body of physical evidence from other sources, which has been satisfactorily rationalized in terms of proposals made by Franck and Meyer.[2] Taken together, the diffraction observations and data in the literature are mutually augmentative and strongly favor a ring-hexamer theory. Models consisting mainly of open-chain species, on the other hand, appear incapable of being brought into satisfactory accord with experimental observations. The dimer[31] could not be detected in this study, but might be observable in a room-temperature electron-diffraction experiment if the working HF pressure were reduced to ~200 torr.

Structural features of the hexameric rings are summarized as follows: The hydrogen-bonded FF distances are comparable with those found in the crystal. *Mean* FFF angles found by gas electron diffraction are roughly 16° smaller than the 120° angles in crystalline chains, but this difference may be due to thermal puckering of the extremely flexible skeletal ring in the vapor phase. There is some indication that the distribution of protons observed in the polymer structure is not adequately describable in terms of the usual simple one-dimensional double-minimum potential model.

[31] D. F. Smith, J. Mol. Spectry. **3**, 473 (1959).

THE JOURNAL OF CHEMICAL PHYSICS VOLUME 50, NUMBER 8 15 APRIL 1969

Low-Energy Electron-Diffraction Studies of the Interaction of Oxygen with a Molybdenum (100) Surface*

H. K. A. KAN AND S. FEUERSTEIN

Aerospace Corporation, El Segundo, California

(Received 5 August 1968)

Oxygen adsorption on the (100) surface of molybdenum single crystals was examined by low-energy electron-diffraction (LEED) in a display-type apparatus. Continuous diffraction-pattern observations from an initially clean surface were made at reaction temperatures between room temperature and 850°C. Below 650°C, no new ordered structures were observed. At 750°C, four ordered structures were formed on the surface with increasing oxygen coverage. The thermal characteristics and kinetics of formation of these oxides are discussed. In addition, models of surface structure with less than a monolayer oxygen coverage are presented.

INTRODUCTION

The interaction of oxygen with molybdenum has been studied extensively in the past, but little is known about the details of the initial stage of the oxidation process. Low-energy electron-diffraction (LEED) techniques are particularly well suited for the study of gas adsorption in the monolayer region, because the penetration of electrons with energies in the 100-eV range is limited to a few atomic layers. Haas and Jackson[1] have reported a LEED study of the interaction of oxygen with an Mo (110) plane, but, on the whole, relatively few experiments have been carried out on molybdenum single crystals.[2] Moreover, the effect of temperature on surface structure that forms as a result of adsorption is largely unknown. The studies reported here utilize low-energy electron diffraction to examine continuously the reaction of oxygen with an Mo (100) surface at different temperatures. Emphasis is on the effect of temperature on the formation of ordered surface structures as a result of oxygen adsorption. Diffraction patterns were observed continuously at the reaction temperature.

* This work was supported by the U.S. Air Force under Contract No. F04695-67-C-0158.

[1] T. W. Haas and A. G. Jackson, J. Chem. Phys. **44**, 2921 (1966).

[2] Since the completion of the manuscript, an article appeared in the literature [K. Hayek, H. E. Farnsworth, and R. L. Park, Surface Sci. **10**, 429 (1968)] which in part deals with the present subject. Their observation of cleaning procedure by heating and the room-temperature interaction of clean Mo (100) with oxygen is in agreement with ours. The main results described here on the reaction observed at elevated temperatures can be considered complementary to their work since the experimental conditions are entirely different.